Demand Side Management in A Day-Ahead Wholesale Market: A Comparison of Industrial & Social Welfare Approaches

Bo Jiang, Amro M. Farid, Kamal Youcef-Toumi

Abstract

The intermittent nature of renewable energy has been discussed in the context of the operational challenges that it brings to electrical grid reliability. Demand Side Management (DSM) with its ability to allow customers to adjust electricity consumption in response to market signals has often been recognized as an efficient way to mitigate the variable effects of renewable energy as well as to increase system efficiency and reduce system costs. However, the academic & industrial literature have taken divergent approaches to DSM implementation. While the popular approach among academia adopts a social welfare maximization formulation, the industrial practice compensates customers according to their load reduction from a predefined electricity consumption baseline that would have occurred without DSM. This paper rigorously compares these two different approaches in a day-ahead wholesale market context analytically and in a test case using the same system configuration and mathematical formalism. The comparison of the two models showed that a proper reconciliation of the two models might make them mitigate the stochastic netload in fundamentally the same way, but only under very specific conditions which are rarely met in practice. While the social welfare model uses a stochastic net load composed of two terms, the industrial DSM model uses a stochastic net load composed of three terms including the additional baseline term. DSM participants are likely to manipulate the baseline in order to receive greater financial compensation. An artificially inflated baseline is shown to result in a different resources dispatch, high system costs, and unachievable social welfare, and likely requires more control activity in subsequent layers of enterprise control.

NOMENCLATURE

GC	subscript for dispatchable (controllable) generators (e.g. thermal plants)
GS	subscript for stochastic generators (e.g. wind, solar photo-voltaic)
DC	subscript for dispatchable (controllable) demand units (i.e. participating in DSM)
DS	subscript for stochastic demand units (i.e. conventional load)
i	index of dispatchable generators
j	index of dispatchable demand unit
k	index of stochastic generators
l	index of stochastic demand unit
t	index of unit commitment time intervals
N_{GC}	Number of dispatchable generators
N_{DC}	Number of dispatchable demand units
N_{GS}	Number of stochastic generators
N_{DS}	Number of stochastic demand units
T	Number of unit commitment time intervals
$\mathcal{W}$	social welfare
P_{GCit}	dispatched power generation at the i^{th} dispachable generator in the t^{th} time interval

Bo Jiang is with the Mechanical Engineering at the Massachusetts Institute of Technology, Cambridge, MA, USA. bojiang@mit.edu
Amro M. Farid is an Associate Professor of Engineering with the Thayer School of Engineering at Dartmouth, Hanover, NH, USA. He is also a Research Affiliate with the MIT Mechanical Engineering Department. amfarid@dartmouth.edu, amfarid@mit.edu
Kamal Youcef-Toumi is a Professor of Mechanical Engineering at the Massachusetts Institute of Technology, Cambridge, MA, USA. youcef@mit.edu

P_{DCjt}	dispatched power consumption at the j^{th} dispatchable demand unit in the t^{th} time interval
$\hat{P}_{DCjt}$	forecasted power consumption of the j^{th} dispatchable demand unit in the t^{th} time interval
$\tilde{P}_{DCjt}$	baseline power consumption of the j^{th} dispatchable demand unit in the t^{th} time interval
$\hat{P}_{GSkt}$	forecasted power generation at the k^{th} stochastic generator in the t^{th} time interval
$\hat{P}_{DSlt}$	forecasted power consumption of the l^{th} stochastic demand unit in the t^{th} time interval
$\underline{P_{GCi}}$	min. capacity of the i^{th} dispatchable generator
$\underline{P_{DCj}}$	min. capacity of the j^{th} dispatchable demand unit
$\underline{R_{GCi}}$	min. ramping capability of the i^{th} dispatchable generator
$\underline{R_{DCj}}$	min. ramping capability of the j^{th} dispatchable demand unit
$\overline{P_{GCi}}$	max. capacity of the i^{th} dispatchable generator
$\overline{P_{DCj}}$	max. capacity of the j^{th} dispatchable demand unit
$\overline{R_{GCi}}$	max. ramping capability of the i^{th} dispatchable generator
$\overline{R_{DCj}}$	max. ramping capability of the j^{th} dispatchable demand unit
$\mathcal{C}_{GCi}$	cost of the i^{th} dispatchable generator
$\mathcal{S}_{GCi}$	startup cost of the i^{th} dispatchable generator
$\mathcal{D}_{GCi}$	shutdown cost of the i^{th} dispatchable generator
$\mathcal{R}_{GCit}$	running cost of the i^{th} dispatchable generator in the t^{th} time interval
A_{GCi}	quadratic cost function coefficient of the i^{th} dispatchable generator
B_{GCi}	linear cost function coefficient of the i^{th} dispatchable generator
ζ_{GCj}	cost function constant of the i^{th} dispatchable generator
$\mathcal{U}_{DCj}$	demand utility of the j^{th} dispatchable demand unit
$\mathcal{S}_{DCj}$	startup utility of the j^{th} dispatchable demand unit
$\mathcal{D}_{DCj}$	shutdown utility of the j^{th} dispatchable demand unit
$\mathcal{R}_{DCjt}$	running utility of the j^{th} dispatchable demand unit in the t^{th} time interval
A_{DCj}	quadratic utility function coefficient of the j^{th} dispatchable demand unit
B_{DCj}	linear utility function coefficient of the j^{th} dispatchable demand unit
ζ_{DCj}	utility function constant of the j^{th} dispatchable demand unit
$\mathcal{C}_{DCj}$	cost of the j^{th} virtual generator
$\mathbb{S}_{DCj}$	startup cost of the j^{th} virtual generator
$\mathbb{D}_{DCj}$	shutdown cost of the j^{th} virtual generator
$\mathbb{R}_{DCjt}$	running cost of the j^{th} virtual generator in the t^{th} time interval
$\mathbb{A}_{DCj}$	quadratic cost function coefficient of the j^{th} virtual generation
$\mathbb{B}_{DCj}$	linear cost function coefficient of the j^{th} virtual generation
ξ_j	cost function constant of the j^{th} virtual generation
w_{GCit}	binary variable for the state of the i^{th} dispatchable generator in the t^{th} time interval
u_{GCit}	binary variable for the startup state of the i^{th} dispatchable generator in the t^{th} time interval
v_{GCit}	binary variable for the shutdown state of the i^{th} generator in the t^{th} time interval
w_{DCjt}	binary variable for the state of the i^{th} dispatchable demand unit in the t^{th} time interval
u_{DCjt}	binary variable for the startup state of the j^{th} dispatchable demand unit in the t^{th} time interval
v_{DCjt}	binary variable for the shutdown state of the j^{th} dispatchable demand unit in the t^{th} time interval
ω_{DCjt}	binary variable for the state of the j^{th} virtual generation in the t^{th} time interval
μ_{DCjt}	binary variable for the startup state of the j^{th} virtual generation at the beginning of the t^{th} time interval
ν_{DCjt}	binary variable for the shutdown state of the j^{th} virtual generation at the beginning of the t^{th} time interval

I. INTRODUCTION

A. Motivation

The intermittent nature of renewable energy has been discussed in the context of the operational challenges that it brings to electrical grid reliability [1]–[3]. The fast fluctuations in renewable energy generation require high ramping capability which must be met by dispatchable energy resources. Additionally, a sudden loss of renewable generation can threaten grid reliability in the absence of adequate generation reserves.

In contrast, Demand Side management (DSM) with its ability to allow customers to adjust electricity consumption in response to market signals has often been recognized as an efficient way to shave load peaks [4]–[7] and mitigate the variable effects of renewable energy [8]–[10]. This work focuses on DSM where end users can change their consumption in response to dynamic changes in electricity price signals [11], rather than static energy efficiency techniques. It increases the bulk electric system flexibility [12], [13] and reliability [7], [13]–[15] by providing additional dispatchable resources which can potentially offset imbalances caused by renewable energy [16], [17]. DSM has also been advocated for its ability to increase system efficiency and reduce system costs [18], [19]. By encouraging customers to adjust their electricity consumption in response to market signals, DSM reduces the need for more expensive generators with high ramping capability. Meanwhile, DSM increases the utilization of generating capacities that would have been otherwise idle during off-peak hours, thus reducing the real cost of renewable integration [20]. The electricity supply side, load-reducing customers and non-load-reducing customers all benefit economically from load reductions [21]–[23].

The deregulation of electricity markets [24]–[28], along with the advances in information and communication technologies [12], [29]–[31], has motivated more active DSM programs. As a result, Independent System Operators (ISOs) and Reliability Transmission Organizations (RTOs) have been implementing DSM for its potential to lower market prices, reduce price volatility, improve customer options, and increase the elasticity from wholesale to retail market [32]. Researches on DSM have addressed the minimization of energy consumption, maximization of customer utility, the minimization of customer discomfort, the stabilization of electricity prices, and multi-objective optimizations from the customer side [33]–[40]. In addition, there have also been studies on the integration of DSM and renewable uncertainty [41], centralized or distributed demand control algorithms [14], [30], [42]–[46], demand-side storage [47], [48], models of customer behavior [49], and prediction of DSM participation potential [50]–[52].

Despite its recognized importance [53]–[55], the industrial and academic literature seem to have taken divergent approaches to DSM implementation. A common approach among academic researchers is to maximize social welfare defined as the net benefits from electricity consumption and generation based on the utility of dispatchable demand [33], [35], [36], [56], [57]. In the meantime, the industrial trend has been to introduce “virtual generators” in which customers are compensated for load reductions from baseline electricity consumption [25], [26], [58]–[62]. Such a baseline is defined as the counterfactual electricity consumption that would have occurred without DSM and is estimated from historical data from the prior year [63]–[65]. The industrial baselines easily involve errors and are most likely to be different from the load forecast. Firstly, the methods of determining the load forecast and industrial baseline are fundamentally different. While the latter is calculated a day in advance based upon sophisticated methods [66], the formulae for baseline are much more basic and determined months in advance [32], [67]–[70]. Indeed, it is conceivable that a baseline is set and then the demand side participant makes (static) long-term energy efficiency improvements and then is compensated for the now guaranteed “load-reduction”. As several authors note, the baseline itself is subject to manipulation because DSM participants have greater awareness of their facilities than the regulatory agencies charged with estimating the baseline [11], [71].

B. Scope

Demand side management has been implemented in many ways: transmission/wholesale versus distribution/retail, direct load control versus incentivized approaches, and normal operation versus emergency operation [18]. Wholesale markets manage generation to transmission, while retail market starts from step-down transformers and distributes electricity to customers on a flat-rate [72]. This work therefore pertains to wholesale economically incentivized normal operation within the day ahead market. The procurement and dispatch decision from the wholesale market is the result of different parties bidding on various time-scales [73] including in the long-term capacity market, the short-term energy market, and the operating reserve market. Energy markets consists of day-ahead energy markets and real-time energy markets. This work is of greatest relevance to American ISOs which have implemented FERC Order 745. For example, PJM ISO has allowed its electricity consumers to participate in energy markets to minimize system costs [73].

The DSM literature is presented as two classes of energy market problems. The first class of problem is the power scheduling in a day-ahead market, without any guarantee that the dispatchable demands will actually consume the allocated power [2], [4], [10], [31], and the second class is the load shifting in real-time market, where the customers are always able to change their consumption patterns [3], [10], [14], [30], [31], [55]. This paper belongs to the first category and focuses on comparing the academic and industrial DSM methods in a day-ahead energy market; presented as a unit commitment problem. The underlying assumption is that despite the errors inherent to renewable energy forecast, the forecast model is reliable for the purpose of day-ahead scheduling, and the errors of renewable energy forecast will be corrected in subsequent layers of control in real-time markets and regulation [74], [75]. The day-ahead energy market mechanism as compared to real-time energy markets is described in detail in Section II-A.

C. Contribution

While the differences between the academic and industrial methods and the errors associated with the baseline have often been a part of policy discussions [11], they have not been rigorously studied. There have been attempts to incorporate the concept of social welfare into the market auction mechanism, but they are based on conventional dispatch giving no consideration to responsive demands or renewables, and thus renders a very different and much simpler case [76]. For a day-ahead scheduling scenario, a unit commitment problem incorporating DSM has been studied simply from the suppliers side to minimize generation costs [77] or to maximize electric power utility profit [78], [79], and from a markets perspective using either the social welfare [80] and industrial method [81]–[83]. This paper aims to rigorously compare the social welfare and the industrial load reduction approaches and study the effects of an erroneous industrial baseline in a day-ahead wholesale market context using the same system configuration and mathematical formalism [84], [85].

D. Paper Outline

The remainder of this paper develops in six sections. Section II summaries highlights from both the academic literature and industrial documents. Section III presents the mathematical models for both the social welfare and industrial methods of unit commitment with dispatchable demands as well as the model reconciliation. In Section IV, the two optimization programs are compared analytically, and the conditions under which the two optimization programs are equivalent are discussed. The test case and methodology are presented in Section V. Section VI presents and discusses the results from the case study for both models with an accurate and erroneous baseline. The paper concludes in Section VII.

II. Background

This section first introduces readers to economic dispatch and unit commitment problems. It then summarizes the two contrasting approaches to demand dispatching: social welfare methods often found in academia and load reduction from baseline methods implemented in industry.

A. Economic Dispatch & Unit Commitment in Wholesale Power Markets

The real-time ISO wholesale market adopts an economic dispatch (ED) problem on the timescale of minutes. Different generating units include nuclear, thermal, hydro, and gas units, and have very different physical limitations and costs characteristics. A traditional ED utilizes all online generating units to meet the total forecast power requirements including customer demands and transmission losses, and allocates the generating power among units such that the total power production costs are minimized [86]. Therefore, a traditional ED problem consists of minimizing generating cost under the constraint of system power balance and physical limitations of generating units, namely capacity and ramping limits [86]. Here, the costs only include that of running the units at the dispatched levels.

The day-ahead ISO wholesale market adopts a unit commitment problem using time periods of an hour or a few hours. In contrast to an ED problem, the goal of which is to determine the optimal generating level, the primary purpose of UC is to choose the appropriate set of online generating units during each time period for the next-day ED. Instead of assuming all available units online, it needs to determine the online or offline state of units. Limitations exist on the frequency each generating unit can be started up or shut down, and costs are associated with starting up or shutting down units. Therefore, two modifications from ED formalism, at a minimum, are needed to form a UC problem: 1) the on/off state of each unit needs to be consistent with the starting and shutting process of the units. 2) the total costs need to include start-up and shut-down costs in addition to operating costs. [86]

Another difference worth special attention is that while transmission losses explicitly exist in ED, it does so less frequently in UC. The reason is that UC usually dispatches over long time periods and is only based on coarse forecasts and does not provide accurate generating levels. Therefore, the transmission loss is not expected to affect the UC greatly but greatly complicates the optimization, and is usually omitted in UC problems [74], [86]–[91].

B. Academic Literature

A popular approach in the academic literature is to adopt a maximal social welfare problem formulation. Elastic demand is characterized by its utility U – the benefit from electricity consumption, and generation is characterized by its cost C [86]. The maximum social welfare determines the dispatch schedule and price for suppliers and customers at the same time [33], [78]. In an economic dispatch context, social welfare has been defined in textbooks as [86]:

$$SW(P_G, P_D) = \sum_{j=1}^{m} U_j(P_{Dj}) - \sum_{i=1}^{n} C_i(P_{Gi}) \tag{1}$$

where P_D and P_G represent the individual demands and generators respectively; m and n represent the number of demands and generators. Assuming lossless transmission, the system power balance constraint becomes [86]:

$$\sum_{i=1}^{n} P_{Gi} = \sum_{j=1}^{m} P_{Dj} \tag{2}$$

The objective function in (1) and the constraint in (2) constitute the simplest form of social welfare maximization. As mentioned and cited in the introduction, the electricity industry implements a different approach.

C. Industrial Practice

The industrial approach to dispatching demand minimizes the total cost of dispatchable generation and virtual generation. A curtailment service provider (CSP) represents the demand units participating in the wholesale energy market. Each CSP has an "administratively-set" electricity consumption baseline as an estimate of consumption without DSM incentives and from which load reductions are measured. The CSP can participate in one of several wholesale energy markets [92]; one of them being the Day-Ahead Scheduling Reserve Market (DASR) where generation suppliers, load serving entities, and CSPs bid through an ISO/RTO [73]. The bidding process determines the dispatched resources as well as the electricity price for the next day [61]. Accepted load reductions are obliged to commit and are subsidized by ISO/RTO based on the bidding price compared to the Locational Marginal Pricing (LMP) and the Retail Rates (GT) [22]. While very much discouraged, customers have an implicit incentive to surreptitiously inflate the administrative baseline for greater compensation. For example, the customers can artificially increase their electricity consumption when baselines are being evaluated [11]. Customers who anticipate to reduce loads regardless of DSM are also more likely to be attracted to participate [11]. Another example is customers having multiple facilities shift loads between facilities to create false load reductions [11]. Successful baseline manipulation may cause generation relocation and inefficient price information [11].

III. Mathematical Models

This section now describes the mathematical formulation for both the social welfare and industrial load reduction models.

A. Social Welfare Maximization

The formulation of maximal social welfare problem is as follows. Unlike the economic dispatch problem presented in Section II-B, the unit commitment model schedules the dispatchable resources and determines their states over multiple time intervals. The optimization program in Section II-B also assumed that all generators and loads are dispatchable. For greater practicality, this assumption is relaxed so that stochastic generation (i.e. renewable energy) and stochastic demand (i.e. conventional load) can be included. These are taken as fixed exogenous quantities whose costs and utilities are independent from dispatch decisions and which must be balanced by dispatchable generation and demand units. The objective function to maximize is the total social welfare $\mathcal{W}$ is given by [84]:

$$\mathcal{W} = \sum_{t=1}^{T} \left[\sum_{j=1}^{N_{DC}} \mathcal{U}_{DCj}(P_{DCjt}) - \sum_{i=1}^{N_{GC}} \mathcal{C}_{GCi}(P_{GCit}) \right] \tag{3}$$

where both the demand utility $\mathcal{U}_{DCj}$ and generation cost $\mathcal{C}_{GCi}$ have a startup, a shutdown, and a running component shown in Equation (4) and Equation (5) [84].
$\forall i = 1, ..., N_{GC}, \forall j = 1, ..., N_{DC}, \forall t = 1, ..., T:$

$$\mathcal{C}_{GCi}(P_{GCit}) = u_{GCit}(\mathcal{S}_{GCi}) + v_{GCit}(\mathcal{D}_{GCi}) + w_{GCit}\left[\mathcal{R}_{GCi}(P_{GCit})\right] \tag{4}$$

$$\mathcal{U}_{DCj}(P_{DCjt}) = u_{DCjt}(\mathcal{S}_{DCj}) + v_{DCjt}(\mathcal{D}_{DCj}) + w_{DCjt}\left[\mathcal{R}_{DCj}(P_{DCjt})\right] \tag{5}$$

where the running cost for generators $\mathcal{R}_{GCit}$ and running utility for demands $\mathcal{R}_{DCjt}$ are modeled as quadratic functions to capture the change in marginal costs and marginal utilities [84].
$\forall i = 1, ..., N_{GC}, \forall j = 1, ..., N_{DC}, \forall t = 1, ..., T:$

$$\mathcal{R}_{GCi}(P_{GCit}) = A_{GCi}(P_{GCit})^2 + B_{GCi}(P_{GCit}) + \zeta_{GCi} \tag{6}$$

$$\mathcal{R}_{DCj}(P_{DCjt}) = A_{DCj}(P_{DCjt})^2 + B_{DCj}(P_{DCjt}) + \zeta_{DCj} \tag{7}$$

Acquiring a reliable utility model in day-ahead wholesale market necessitates accurate forecast of utility functions and is not always easy to achieve in that it depends on customers providing information for the next day. Not only are errors inherent to utility forecast, but the heterogeneity of customers also brings difficulty to curtailment service providers serving aggregated groups of customers. [33] However, it is still considered a good method and used commonly among academic studies for two reasons. Firstly, customers do not have incentives to report false utility information. Remember utility is defined as the benefits a customer gets from consuming electricity, and over-stating utility results in the customer over-buying and wasting money on excess electricity. On the other hand, under-stating utility leads to not procuring enough electricity. Secondly the customers are expected to be well aware of their utility information and one day is a considered a short period in advance and helps to mitigate forecast errors.

The objective function is optimized subject to the system power balance constraint in Equation (8), and the physical capacity constraint for both the dispatchable generators in Equation (9) and dispatchable demands in Equation (10). Equation (8) describes lossless power flow balance. It states that the sum of all generation terms must equal the sum of all demand terms. $\hat{P}_{DSkt}$ and $\hat{P}_{GSlt}$ are forecasted values of their associated stochastic quantities one day in advance. The ramping rate is defined as the change in generation power from the last time interval as in Equation (11a). In a simplified model, the ramping of generators is assumed to be linear. This approximation has been commonly adopted among large-scale electrical grid studies and is described in textbooks [86]. The physical downward and upward generation ramping limits are implemented with the lower and upper constraints as in Equation (11b). Similarly, the ramping constraints of dispatchable demands are found in Equation (12). The logical constraints of dispatchable generators and dispatchable demands are shown in Equations (13) and (14) respectively [84].
$\forall i = 1, ..., N_{GC}, \forall j = 1, ..., N_{DC}, \forall t = 1, ..., T:$

$$\sum_{i=1}^{N_{GC}} P_{GCit} - \sum_{j=1}^{N_{DC}} P_{DCjt} = \sum_{k=1}^{N_{DS}} \hat{P}_{DSkt} - \sum_{l=1}^{N_{GS}} \hat{P}_{GSlt} \tag{8}$$

The power balance constraint is composed of terms: the power injection for the dispatchable and stochastic generating and demand units. As is commonly found in the literature, the power system losses are neglected in UC formalism but compensated by the load following reserves term [74], [86]–[91]. The reader is referred to [93] for one approach to the incorporation of losses. The load following and ramping reserves are calculated for subsequent ED control according to the methods provided in references [74], [75]. In this work, the load following reserve is set to 20% of peakload, a very conservative amount to ensure load tracking in real-time market and imposes no active constraints in the unit commitment problem.

$$w_{GCit} * \underline{P_{GCi}} \leq P_{GCit} \leq w_{GCit} * \overline{P_{GCi}} \tag{9}$$

$$w_{DCjt} * \underline{P_{DCj}} \leq P_{DCjt} \leq w_{DCjt} * \overline{P_{DCj}} \tag{10}$$

The maximum capacity of each dispatchable demand unit is determined one-day ahead using the sophisticated method of load forecasting, contrasted to the industrial baseline which is usually contracted months or even years ahead.

$$R_{GCit} = P_{GCit} - P_{GCi(t-1)} \tag{11a}$$

$$\underline{R_{GCi}} \leq R_{GCit} \leq \overline{R_{GCi}} \tag{11b}$$

$$R_{DCjt} = P_{DCjt} - P_{DCj(t-1)} \tag{12a}$$

$$\underline{R_{DCj}} \leq R_{DCjt} \leq \overline{R_{DCj}} \tag{12b}$$

$$w_{GCit} = w_{GCi(t-1)} + u_{GCit} - v_{GCit} \tag{13}$$

$$w_{DCjt} = w_{DCj(t-1)} + u_{DCjt} - v_{DCjt} \tag{14}$$

B. Industrial Practice: Cost Minimization with Demand Baseline

The formulation of the industrial Unit Commitment model is as follows. Much like the social welfare model, the industrial unit commitment model determines the setpoints for all dispatchable resources. In contrast, however, the optimization goal industrial approach is to minimize the total cost of dispatchable generators and virtual generators over all time intervals of the SCUC period, where the cost of virtual generation is the compensation paid to the customers for reducing their consumption from predefined demand baseline. The industrial demand side mangement objective is given in Equation (15) [84].

$$\sum_{t=1}^{T}\left[\sum_{i=1}^{N_{GC}} \mathcal{C}_{GCi}(P_{GCit}) + \sum_{j=1}^{N_{DC}} \mathcal{C}_{DCj}(\tilde{P}_{DCjt} - P_{DCjt})\right] \tag{15}$$

where the costs of the dispatchable generation remain the same as in Equation (4) and the costs of dispatchable demand shown in Equation (16) [84] also have startup, shutdown, and running cost.
$\forall i = 1, ..., N_{GC}, \forall j = 1, ..., N_{DC}, \forall t = 1, ..., T :$

$$\mathcal{C}_{DCj}(\tilde{P}_{DCjt} - P_{DCjt}) = \mu_{DCjt}(\mathbb{S}_{DCj}) + \nu_{DCjt}(\mathbb{D}_{DCj}) + \omega_{DCjt}\left[\mathbb{R}_{DCj}\right] \tag{16}$$

The running cost is similarly modeled as a quadratic function of the load reduction from the baseline.
$\forall i = 1, ..., N_{GC}, \forall j = 1, ..., N_{DC}, \forall t = 1, ..., T :$

$$\mathbb{R}_{DCj}(\tilde{P}_{DCjt} - P_{DCjt}) = \mathbb{A}_{DCj}(\tilde{P}_{DCjt} - P_{DCjt})^2 + \mathbb{B}_{DCj}(\tilde{P}_{DCjt} - P_{DCjt}) + \xi_{DCj} \tag{17}$$

The objective function is optimized subject to same system power balance constraint in Equation (8) [84]. Both the dispatchable generation and virtual generation are subject to the capacity limits in Equations (9) and (18) respectively, the ramping limits in Equations (11) and (12) respectively, and the logical constraints in Equations (13) and (19) respectively [84].
$\forall j = 1, ..., N_{DC}, \forall t = 1, ..., T$

$$\begin{aligned} \omega_{DCjt} * \underline{\tilde{P}_{DCjt} - P_{DCjt}} &\leq \tilde{P}_{DCjt} - P_{DCjt} \\ \tilde{P}_{DCjt} - P_{DCjt} &\leq \omega_{DCjt} * \overline{\tilde{P}_{DCjt} - P_{DCjt}} \end{aligned} \tag{18}$$

$$\overline{w}_{DCjt} = \overline{u}_{DCj(t-1)} + \overline{u}_{DCjt} - \overline{v}_{DCjt} \tag{19}$$

The industrial method dictates that the load reduction does not exceed the baseline. A full reduction corresponds to the magnitude of the baseline. As mentioned in Section I & III-A, the baselines are determined months or even years ahead based on electricity consumption history data and are subject to manipulation, and therefore are more prone to errors than its counterpart of maximum dispatchable demand forecast in social welfare model.

C. Model Reconciliation

For fair comparison of the two models, the constraints and utility/cost functions of dispatchable demands in the two models need to be reconciled. The virtual generation cost function in the industrial model is reconciled with the utility function of the corresponding dispatchable demand unit such that the loss in utility in the SW model is equal to the change in virtual generation cost. The economics rationale for this is that the customers are only willing to cut down electricity consumption if their marginal loss in utility is subsidized by the marginal cost in virtual generation [84].
$\forall j = 1, ..., N_{DC}$:

$$-\mathcal{U}_{DCj}(P_{DCj}) + \mathcal{U}_{DCi}(P_{DCj} + \delta P_{DCj}) = \mathcal{C}_{DCj}(\tilde{P}_{DCj} - P_{DCj}) - \mathcal{C}_{DCj}(\tilde{P}_{DCj} - P_{DCj} - \delta P_{DCj}) \tag{20}$$

The dispatchable and virtual generation cost functions (in Equations 6 and 17) and dispatchable demand utility functions (in Equation 7) are substituted into Equation (20). Rearranging quadratic and linear terms yields Equation (21) [84]. Interested readers are referred to reference [84] for further details on this derivation. It shows that the cost function of load reduction is dependent on the choice of baseline.
$\forall j = 1, ..., N_{DC}$:

$$\begin{aligned} \mathbb{A}_j &= -A_j \\ \mathbb{B}_j &= 2 * A_j * \tilde{P}_{DCj} + B_j \end{aligned} \tag{21}$$

The maximum load reduction is assumed to occur when dispatchable demand is operating at its minimum level. Now that the two optimization programs are well defined and reconciled with each other, the next section proceeds to comparing them with each other.

IV. Analytical Comparison of the Two Optimization Models

In this section, the social welfare maximization method and load reduction optimization method are compared analytically using the function reconciliation developed in Subsection III-C. As a conclusion, the two models are shown to yield different optima in all but a few cases. The equivalence conditions require that the industrial baseline is equal to the maximum capacity and that the dispatchable demand startup and shutdown costs are ignored. However, these conditions are seldom true, and therefore the two models will very likely generate different results in practice. The analytical comparison is conducted in two steps first as an economic dispatch problem in Subsection IV-A then as a unit commitment problem in Subsection IV-B.

A. Analytical Comparison in Economic Dispatch

This subsection compares the two models in an economic dispatch scenario where only one time interval is analyzed. Ramping limits and binary variable logical constraints span multiple time intervals. They are neglected here but reintroduced in subsequent sections. The Lagrangian functions for social welfare and industrial programs are presented in Subsubsection IV-A1 and IV-A2 respectively. They are compared in Subsubsection IV-A3 and found to be equivalent if and only if the industrial baseline is equal to the maximum capacity in social welfare model.

1) Social Welfare Model Lagrangian Function: In an economic dispatch problem, the social welfare model reduces to the maximization of total social welfare over all time intervals in Equation (3) to the maximization on one time interval:

$$\sum_{j=1}^{N_{DC}} \mathcal{U}_{DCj}(P_{DCjt}) - \sum_{i=1}^{N_{GC}} \mathcal{C}_{GCi}(P_{GCit}) \tag{22}$$

subject to the power balance equality constraint for all generators and dispatchable demands;

$$\sum_{i=1}^{N_{GC}} P_{GCit} - \sum_{j=1}^{N_{DC}} P_{DCjt} = \sum_{k=1}^{N_{DS}} \hat{P}_{DSkt} - \sum_{l=1}^{N_{GS}} \hat{P}_{GSlt} \tag{23}$$

and the capacity inequality constraints
$\forall i = 1, ..., N_{GC}, \forall j = 1, ..., N_{DC}$:

$$\underline{P_{DCj}} \leq P_{DCjt} \leq \overline{P_{DCj}} \tag{24a}$$

$$\underline{P_{GCi}} \leq P_{GCit} \leq \overline{P_{GCi}} \tag{24b}$$

The Lagrangian function of the social welfare model can then be written as

$$\begin{aligned} L(P_{DCjt}, P_{GCit}, \lambda) = \sum_{i=1}^{N_{GC}} A_{GCi}(P_{GCit})^2 + \sum_{i=1}^{N_{GC}} B_{GCi}(P_{GCit}) + \sum_{i=1}^{N_{GC}} \zeta_{GCi} \\ - \sum_{j=1}^{N_{DC}} A_{DCj}(P_{DCjt})^2 - \sum_{j=1}^{N_{DC}} B_{DCj}(P_{DCjt}) - \sum_{j=1}^{N_{DC}} \zeta_{DCj} \\ -\lambda\Big[\Big(\sum_{i=1}^{N_{GC}} P_{GCit} - \sum_{j=1}^{N_{DC}} P_{DCjt}\Big) - \Big(\sum_{k=1}^{N_{DS}} \hat{P}_{DSkt} - \sum_{l=1}^{N_{GS}} \hat{P}_{GSlt}\Big)\Big] \\ -\mu_1(P_{GCit} - \overline{P_{GCi}}) - \mu_2(P_{GCit} - \underline{P_{GCi}}) - \mu_3(P_{DCjt} - \overline{P_{DCj}}) - \mu_4(P_{DCjt} - \underline{P_{DCj}}) \end{aligned} \tag{25}$$

The optimal solution can be solved from the system of equations in (26) by equating the partial derivative of each variable to zero (Equation (26a) - (26c)) and including the complementary equations for all inequality constraints (Equation (26d) - (26g)):
$\forall i = 1, ..., N_{GC}, \forall j = 1, ..., N_{DC}, \forall t = 1, ..., T :$

$$\frac{\partial L}{\partial P_{GCit}} = 2A_{GCi}P_{GCit} + B_{GCi} - \lambda - \mu_1 - \mu_2 = 0 \tag{26a}$$

$$\frac{\partial L}{\partial P_{DCjt}} = -2A_{DCj}P_{DCjt} - B_{DCj} + \lambda - \mu_3 - \mu_4 = 0 \tag{26b}$$

$$\Big(\sum_{i=1}^{N_{GC}} P_{GCit} - \sum_{j=1}^{N_{DC}} P_{DCjt}\Big) - \Big(\sum_{k=1}^{N_{DS}} \hat{P}_{DSkt} - \sum_{l=1}^{N_{GS}} \hat{P}_{GSlt}\Big) = 0 \tag{26c}$$

$$\mu_1(P_{GCit} - \overline{P_{GCi}}) = 0, \qquad \mu_1 \leq 0 \tag{26d}$$

$$\mu_2(P_{GCit} - \underline{P_{GCi}}) = 0, \qquad \mu_2 \geq 0 \tag{26e}$$

$$\mu_3(P_{DCjt} - \overline{P_{DCj}}) = 0, \qquad \mu_3 \leq 0 \tag{26f}$$

$$\mu_4(P_{DCjt} - \underline{P_{DCj}}) = 0, \qquad \mu_4 \geq 0 \tag{26g}$$

2) Industrial Model Lagrangian Function: Similarly, the industrial model reduces the minimization of total costs over all time intervals in Equation (15) to the minimization of costs on one interval:

$$\sum_{i=1}^{N_{GC}} \mathcal{C}_{GCi}(P_{GCit}) + \sum_{j=1}^{N_{DC}} \mathcal{C}_{DCj}(\tilde{P}_{DCj} - P_{DCjt}) \tag{27}$$

subject to the same power balance constraint as in Equation (23) and capacity limits
$\forall i = 1, ..., N_{GC}, \forall j = 1, ..., N_{DC}, \forall t = 1, ..., T :$

$$\begin{aligned} \underline{P_{GCi}} \leq P_{GCit} \leq \overline{P_{GCi}} \\ \underline{\tilde{P}_{DCj} - P_{DCj}} \leq \tilde{P}_{DCj} - P_{DCjt} \leq \overline{\tilde{P}_{DCj} - P_{DCj}} \end{aligned} \tag{28}$$

The Lagrangian function for the industrial optimization is then written as

$$\begin{aligned} L_(P_{DCjt}, P_{GCit}) = \sum_{i=1}^{N_{GC}} A_{GCi}(P_{GCit})^2 + \sum_{i=1}^{N_{GC}} B_{GCi}(P_{GCit}) + \sum_{i=1}^{N_{GC}} \zeta_{GCi} \\ + \sum_{j=1}^{N_{DC}} \mathbb{A}_{DCj}(\tilde{P}_{DCjt} - P_{DCjt})^2 + \sum_{j=1}^{N_{DC}} \mathbb{B}_{DCj}(\tilde{P}_{DCjt} - P_{DCjt}) + \sum_{j=1}^{N_{DC}} \xi_{DCj} \\ -\lambda\Big[\Big(\sum_{i=1}^{N_{GC}} P_{GCit} - \sum_{j=1}^{N_{DC}} P_{DCjt}\Big) - \Big(\sum_{k=1}^{N_{DS}} \hat{P}_{DSkt} - \sum_{l=1}^{N_{GS}} \hat{P}_{GSlt}\Big)\Big] - \mu_1(P_{GCit} - \overline{P_{GCi}}) - \mu_2(P_{GCit} - \underline{P_{GCi}}) \\ -\mu_3\Big[(\tilde{P}_{DCj} - P_{DCjt}) - \overline{\tilde{P}_{DCj} - P_{DCj}}\Big] - \mu_4\Big[(\tilde{P}_{DCj} - P_{DCjt}) - \underline{\tilde{P}_{DCj} - P_{DCj}}\Big] \end{aligned} \tag{29}$$

The optimal solution can be obtained by equating the partial derivative of Lagrangian function with respect to each variable to zero and solving the complementary conditions simultaneously. Substituting the reconciled virtual generation cost function coefficients Equation (21) into the partial derivative of the Lagrangian function with respect to the dispatchable generation levels yields Equations 30:

$$\frac{\partial L_2}{\partial P_{DCjt}} = 2\mathbb{A}_{DCj}(\tilde{P}_{DCj} - P_{DCjt}) + \mathbb{B}_{DCj} + \lambda - \mu_{1j} + \mu_{2j} = 0 \tag{30}$$

The resulting system of equations required to find the industrial optimal solution is:
$\forall i = 1, ..., N_{GC}, \forall j = 1, ..., N_{DC}, \forall t = 1, ..., T:$

$$\frac{\partial L}{\partial P_{GCit}} = 2A_{GCi}P_{GCit} + B_{GCi} - \lambda - \mu_1 - \mu_2 = 0 \tag{31a}$$

$$\frac{\partial L}{\partial P_{DCjt}} = -2A_{DCj}P_{DCjt} - B_{DCj} + \lambda + \mu_3 + \mu_4 = 0 \tag{31b}$$

$$\Big(\sum_{i=1}^{N_{GC}} P_{GCit} - \sum_{j=1}^{N_{DC}} P_{DCjt}\Big) - \Big(\sum_{k=1}^{N_{DS}} \hat{P}_{DSkt} - \sum_{l=1}^{N_{GS}} \hat{P}_{GSlt}\Big) = 0 \tag{31c}$$

$$\mu_1(P_{GCit} - \overline{P_{GCi}}) = 0, \qquad \mu_1 \leq 0 \tag{31d}$$

$$\mu_2(P_{GCit} - \underline{P_{GCi}}) = 0, \qquad \mu_2 \geq 0 \tag{31e}$$

$$\mu_3\Big[(\tilde{P}_{DCj} - P_{DCjt}) - \overline{\tilde{P}_{DCj} - P_{DCj}}\Big] = 0, \qquad \mu_3 \leq 0 \tag{31f}$$

$$\mu_4\Big[(\tilde{P}_{DCj} - P_{DCjt}) - \underline{\tilde{P}_{DCj} - P_{DCj}}\Big] = 0, \qquad \mu_4 \geq 0 \tag{31g}$$

3) Equivalance Conditions: Equations (26) and Equation (31) are then compared. A close inspections shows that Equations (26a) to (26e) are the same as their industrial model counterparts in Equations (31a) to (31e). Equation (26a-b) and (31a-b) are identical if written with respect to the same decision variables and same utility and cost function coefficients. This implies that the objective functions are the same for the two models given proper reconciliation. Equation (26c) and (31c) result in identical form of power balance after baseline cancellation. Equation (26c-d) and (31c-d) are in identical form despite in different models because they come from the unvaried physical limit on dispatchable generators. Furthermore, Equation (26f)&(26g) are equivalent to Equation (31f)&(31g) if the conditions in Equation (32) are met.
$\forall i = 1, ..., N_{GC}, \forall j = 1, ..., N_{DC}, \forall t = 1, ..., T:$

$$\tilde{P}_{DCj} - \underline{\tilde{P}_{DCj} - P_{DCjt}} = \overline{P_{DCj}} \tag{32a}$$

$$\tilde{P}_{DCj} - \overline{\tilde{P}_{DCj} - P_{DCj}} = \underline{P_{DCj}} \tag{32b}$$

In other words, the two optimization programs are the same if and only if the industrially defined minimum load reduction $\underline{\tilde{P}_{DCj} - P_{DCjt}}$ occurs at the highest dispatchable demand level in the social welfare model $\overline{P_{DCj}}$, and the highest load reduction $\overline{\tilde{P}_{DCj} - P_{DCj}}$ occurs at the lowest dispatchable demand level in the social welfare model $\underline{P_{DCj}}$.

If it is assumed that the minimum reduction $\underline{\tilde{P}_{DCj} - P_{DCjt}}$ is zero when the customers do not reduce their electricity consumption. Equation (32a) simplifies to (33a).
$\forall i = 1, ..., N_{GC}, \forall j = 1, ..., N_{DC}, \forall t = 1, ..., T:$

$$\tilde{P}_{DCj} = \overline{P_{DCj}} \tag{33a}$$

$$\tilde{P}_{DCj} - \overline{\tilde{P}_{DCj} - P_{DCj}} = \underline{P_{DCj}} \tag{33b}$$

With the above assumption, if the coefficients are properly reconciled as in Equation (21), the two optimization programs are equivalent if the baseline is equal to the maximum capacity in the social welfare model (Equation (33a)), and the maximum load reduction occurs when the dispatchable demand is running at its minimum level (Equation (33b)).

B. Analytical Comparison in Unit Commitment

This subsection now returns to the comparison of the models as unit commitment problems. The optimal solution in social welfare maximization model is proved to minimize the total costs in the industrial model, rather than solving the two models explicitly.

First, the startup and shutdown costs of dispatchable demands have completely different physical meanings in the two optimization programs and including them in the optimization will result in different dispatch levels from the two models. In the social welfare model, the startup cost and shutdown cost represent the costs to turn the corresponding load facility on and off respectively. However, in the industrial model, the startup cost occurs when load reduction starts from the baseline, and the shutdown cost occurs when the load returns to the baseline from a lower consumption level. Therefore, only when the startup and shutdown costs are ignored can the equivalence conditions in Equation (33) be extended to unit commitment.

With this insight in mind, ramping and logical constraints can be addressed for the two models. The solutions in the social welfare model are always feasible in the industrial model if Equation (33) is met, and vice versa. Intuitively, the two models should have the same results because the social welfare loss from the optimal point in social welfare model equals the additional cost in the industrial model. Let P^*_{GCit} and P^*_{DCjt} denote the optimal solution in the social welfare problem and P_{GCit} and P_{DCjt} be any other dispatch level. Symbolically,

$$\mathcal{W}(P^*_{GCit}, P^*_{DCjt}) - \mathcal{W}(P_{GCit}, P_{DCjt}) \geq 0 \tag{34}$$

If the optimal point also yields the minimum total system costs then two model are equivalent under the previously described conditions.

Substituting the social welfare definition in Equation (3) and the dispatchable demand utility functions in Equation (5)&(7) into Equation (34) and eliminating all dispatchable demand startup and shutdown costs gives

$$\sum_{t=1}^{T}\sum_{j=1}^{N_{DC}}\Big[A_{DCj}({P^*_{DCjt}}^2 - {P_{DCjt}}^2) + B_{DCj}(P^*_{DCjt} - P_{DCjt})\Big] - \sum_{t=1}^{T}\sum_{i=1}^{N_{GC}}\Big[\mathcal{C}_{GCi}(P^*_{GCit}) - \mathcal{C}_{GCi}(P_{GCit})\Big] \geq 0 \tag{35}$$

Turning to the industrial load reduction method, the difference in total system costs between the social optimal point and any other point is

$$\sum_{t=1}^{T}\Big[\sum_{i=1}^{N_{GC}}\mathcal{C}_{GCi}(P^*_{GCit}) + \sum_{j=1}^{N_{DC}}\mathcal{C}_{DCj}(\tilde{P}_{DCj} - P^*_{DCjt})\Big] - \sum_{t=1}^{T}\Big[\sum_{i=1}^{N_{GC}}\mathcal{C}_{GCi}(P_{GCit}) + \sum_{j=1}^{N_{DC}}\mathcal{C}_{DCj}(\tilde{P}_{DCj} - P_{DCjt})\Big] \tag{36}$$

Similarly, substituting in the cost of virtual generation in Equation (16 & 17) and eliminating virtual generation startup and shutdown cost gives

$$\begin{aligned}&\sum_{t=1}^{T}\sum_{i=1}^{N_{GC}}\Big[\mathcal{C}_{GCi}(P^*_{GCit}) - \mathcal{C}_{GCi}(P_{GCit})\Big] \\ &+ \sum_{t=1}^{T}\sum_{j=1}^{N_{DC}}\Big[\mathbb{A}\Big((\tilde{P}_{DCj} - P^*_{DCjt})^2 - (\tilde{P}_{DCj} - P_{DCjt})^2\Big) + \mathbb{B}\Big((\tilde{P}_{DCj} - P^*_{DCjt}) - (\tilde{P}_{DCj} - P_{DCjt})\Big)\Big]\end{aligned} \tag{37}$$

Substituting in the reconciled coefficients in Equation (21) results in the negative of the social welfare optimal solution condition in Equation (35), so

$$\sum_{t=1}^{T}\Big[\sum_{i=1}^{N_{GC}}\mathcal{C}_{GCi}(P^*_{GCit}) + \sum_{j=1}^{N_{DC}}\mathcal{C}_{DCj}(\tilde{P}_{DCj} - P^*_{DCjt})\Big] - \sum_{t=1}^{T}\Big[\sum_{i=1}^{N_{GC}}\mathcal{C}_{GCi}(P_{GCit}) + \sum_{j=1}^{N_{DC}}\mathcal{C}_{DCj}(\tilde{P}_{DCj} - P_{DCjt})\Big] \leq 0 \tag{38}$$

This means that P^*_{DCjt} and P^*_{DCjt} always have less system costs. In other words, the social welfare optimal dispatch level is also the industrial optimal solution.

In summary, the two models are only equivalent under specific conditions; namely the startup and shutdown costs of dispatchable demands have to be neglected, the minimum and maximum load reduction occur when the dispatchable demand unit is running at its maximum and minimum capacity in the social welfare respectively. Not meeting these conditions will result in different dispatch levels from the two models.

V. Case Study Methodology

The case study consists of a day-ahead unit commitment simulation in a wholesale market for both the social welfare and industrial DSM methods. For fairness of comparison, the same system configuration and data are used to compare the two optimization programs presented in the previous section. The results are studied for their differences in the dispatched energy resources, resulting social welfare, and system costs. Data is drawn from the *Reliability Test System(RTS)-1996* [94], [95] and the Bonneville Power Administration (BPA) website [96], [97]. The following subsections describe the simulation parameters in detail.

A. Time Scale

In the study of a day-ahead UC program, the time span is 24 hours. A 1-hour time interval is chosen for the case study [84].

B. Stochastic Generation, Stochastic Demand

The stochastic generation is taken as the renewable energy generation [84]. Because it only appears in the power system balance constraint, only aggregate renewable energy generation is required. It is drawn from the wind forecast data published on the Bonneville Power Administration (BPA) website for May 12, 2013 [97]. The test case presented in this paper draws upon two different sources RTS-96 and BPA database due to availability. In order for them to design a sensible case which demonstrates the many phenomena presented in the paper, the load and wind data was scaled up to 1.6 times of its value to match the RTS-96 test case. The raw data for the load forecast has a sampling resolution of 5 minutes, and was down sampled by taking hourly averages. The resulting numbers are provided in Table I.

Similarly, the stochastic demand is taken as the conventional load [84]. Its aggregate value is drawn from the BPA load repository for the same day [96], scaled by the same factor, and downsampled to an hourly resolution. The resulting numbers are provided in Table I and only apply to the demand side units not participating in the DSM program.

TABLE I
Stochastic Demand and Generation Levels in MW [96], [97]

Hour of the Day	1	2	3	4	5	6	7	8	9	10	11	12
Load Forecast 05/15/2013 (MW)	8347	8036	7795	7691	7711	7827	7994	8487	9186	9515	9626	9648
Wind Forecast 05/15/2013 (MW)	3163	2528	2518	2861	3037	2878	3231	3576	3320	3242	3471	3335
Hour of the Day	13	14	15	16	17	18	19	20	21	22	23	24
Load Forecast 05/15/2013 (MW)	9679	9618	9594	9621	9657	9701	9728	9753	9927	9753	9132	8498
Wind Forecast 05/15/2013 (MW)	3343	3623	4009	4522	4716	5028	4360	4253	3412	2421	2136	2160

C. Dispatchable Generation,Dispatchable Demands, & Demand Baseline

Dispatchable generators refer to the generation plants that can be fully controlled. Their dispatch level is a key quantity of interest in this study. Dispatchable demands come from the DSM participants and are assumed to be fully controllable without error.

Dispatchable generator parameters are listed in Table II [94]. The startup cost is based on hot start. Slack generators, regulating generators and hydro generators do not participate in unit commitment, and therefore are excluded from the table. The system has a total dispatchable generating capacity of 8424 MW available for day-ahead unit commitment. Ramping is assumed to occur during the first five minutes of every hour.

For the sake of simplicity, a dispatachable demand unit was assumed to exist on each bus [84]. The utility function coefficients for all the dispatchable demand units are assumed to be equal and time-invariant. They are provided in Table III. The minimum and maximum capacity limit of each dispatchable demand unit is assumed to be zero and 9.6% of the peak load published for that bus in the RTS-1996 test case. It is assumed that each dispatchable demands needs 20 minutes to fully ramp between zero and maximum consumption. No load recovery is considered because the customers are assumed to base their electricity consumption only on the current utility and electricity cost. As mentioned in Subsection IV-B, the startup and shutdown costs have entirely different physical meanings in the social welfare and industrial DSM models. For fairness of comparison, the startup and shutdown costs are neglected (i.e. set to zero) in this case study.

This work sets the true baseline to a time-invariant value equal to 9.6% of the peak demand [84]. Furthermore, this work assumes this error-free baseline is equal to the maximum capacity of the dispatchable demand unit in the social welfare model. $\tilde{P}_{DCj} = \overline{P}_{DCj}$. The erroneous baseline was set to 120% of its true value to emphasize its impact [85]. This has the implicit effect of allowing demand units to have a maximum load reduction (capacity) of 120% as that found in the social welfare model.

TABLE II
DISPATCHABLE GENERATOR PARAMETERS [94], [95]

N_{GC}	72									
Unit Type	Generator Index	$\overline{P_{GCi}}$ (MW)	$\underline{P_{GCi}}$ (MW)	$\overline{R_{GCi}}$ (MW/MI)	$\underline{R_{GCi}}$ (MW/MI)	ζ_{GCi} (\$)	B_{GCi} (\$/MW)	A_{GCi} (\$/MW^2)	S_{GCi} (\$)	D_{GCi} (\$)
U12	16,17,18,19,20,49,50,51,52,53,82,83,84,85,86	12	2.4	1	-1	37.8	26.8	10	874	0
U20	01,02,05,06,34,35,38,39,67,68,71,72	20	4.0	3	-3	163.3	39.2	10	115	0
U76	03,04,07,08,36,37,40,41,69,70,73,74	76	15.2	2	-2	151.2	13.5	3	1401	0
U100	09,11,42,44,75,77	100	20.0	7	-7	312.8	21.7	0.1	5750	0
U155	21,22,31,32,54,55,64,65,87,88,97,98	155	31.0	3	-3	210.4	11.0	0.1	611	0
U197	45,46,47,78,79,80	197	39.4	3	-3	315.1	21.9	0.01	10189	0
U350	33,66,99	350	70.0	4	-4	181.0	11.0	0.01	4500	0
U400	23,24,56,57,89,90	400	80.0	20	-20	343.7	5.6	0.01	4700	0

TABLE III
DISPATCHABLE DEMAND UNIT PARAMETERS

index	$\underline{P_{DCj}}$ (MW)	$\overline{R_{DCj}}$ (MW/MI)	$\underline{R_{DCj}}$ (MW/MI)	ζ(\$)	B_j (\$/MW)	A_j (\$/MW^2)	S_{DCj} (\$)	D_{DCj} (\$)
j	0	$\overline{P_{DCj}}/20$	-$\overline{P_{DCj}}/20$	0	112.5	-0.5	0	0

D. Computational Methods

The optimization is implemented with MATLAB 2014b interfaced with GAMS 24.0. The dispatchable generating units parameters, stochastic demand and generation data are imported from CSV (comma-separated values) files to MATLAB. The dispatchable demand units and scenario parameters are setup in MATLAB from MAT files. All data mentioned above is processed in MATLAB to construct arrays containing coefficients and parameters as in Equation (3) to (21) and write them to GDX file that can be read by GAMS.

The optimization model is programmed and solved in GAMS using CPLEX as the optimization engine since both models presented in this paper are mixed integer quadratic convex programs. A relative tolerance of 10^{-7} was chosen for all optimization problems to ensure convergence. Noting that the two optimization programs presented in Equation (3-14) and (15 - 19) may each be classified as Mixed Integer Quadratically Constrained Programs, and CPLEX [98] is chosen as an appropriate off the shelf solver. The output of GAMS is written to GDX and read by MATLAB.

In summary, the data importing and processing is achieved with MATLAB while the optimization is run by GAMS. It takes approximately 1000 seconds to run each optimization program on a desktop computer with Intel(R) Xeon(R) E5405 @ 2.00GHz processor.

VI. RESULTS & DISCUSSION

A. Accurate Baseline

In this subsection, the two demand side management optimization programs are studied for their dispatch levels assuming an accurate baseline equal to the maximum dispatchable demand level.

Figure 1a and 1b show the dispatch levels of the social welfare and industrial demand side management optimization programs respectively. The solid black line represents stochastic demand level in the social welfare model. Subtracting the stochastic generation from it gives the magenta line: the stochastic net load line in the social welfare model. The sum of dispatchable demand in red and this stochastic net load line must meet the sum of dispatchable generation to achieve power system balance. The purple line in the social welfare model represents the frontier of all the dispatchable demand units consumed at their maximum level (i.e. artificially set to the baseline level in the industrial DSM model).

The mechanics of the industrial DSM model is entirely different. The solid black line still represents the non-participating stochastic demand level. The solid yellow line adds the artificial dispatchable demand baseline to the black line. The subtraction of the stochastic generation in green from the yellow line gives the red line: the stochastic net load in the industrial DSM model. The sum of dispatchable generation in blue and the sum of dispatchable demand in purple must meet this line to achieve power system balance. Interestingly, the magenta line now represents the frontier of all the virtual generators at their maximum load reduction (i.e. virtual generation).

That the stochastic net load line in the social welfare and industrial DSM models are different is an important observation [84]. In the former, it is composed of two terms $\sum_{k=1}^{N_{DS}} \hat{P}_{DSkt} - \sum_{l=1}^{N_{GS}} \hat{P}_{GSlt}$. In the latter, it is composed of the same two terms plus a third $\sum_{k=1}^{N_{DS}} \hat{P}_{DSkt} - \sum_{l=1}^{N_{GS}} \hat{P}_{GSlt} + \sum_{j=1}^{N_{DC}} \tilde{P}_{DCjt}$. Therefore, unless the third terms systematically rejects the errors in the first two terms, it is reasonable to conclude that the stochastic netload line in the industrial DSM model is more error prone than its social welfare counterpart.

Figure 1 represents results from the two different approaches. Note, that as expected, the dispatchable generation and demand levels are the same for the social welfare model in Figure 1(a) as for the industrial model in Figure 1(b). It should be emphasized that instead of simple repetition of dispatch levels, the two figures demonstrate the equivalence between the two models under the condition that the industrial baseline is equal to the maximum dispatchable demand level. The numerical simulation shows that despite the difference in optimization objective and mechanics, the two methods yield the same dispatch levels given an accurate baseline and the reconciliation between the dispatchable demand utility and virtual generation cost functions. This is consistent with the analysis in Section IV-B when the proper reconciliation lead to fundamentally the same optimization problem from two different perspectives. As mentioned in Section II, the dispatched generation line appears to remain relatively constant around 7000MW for much of the day. In the meantime, the dispatchable demand and virtual generation vary substantially from nearly zero to approximately 2000MW over the course of the day.

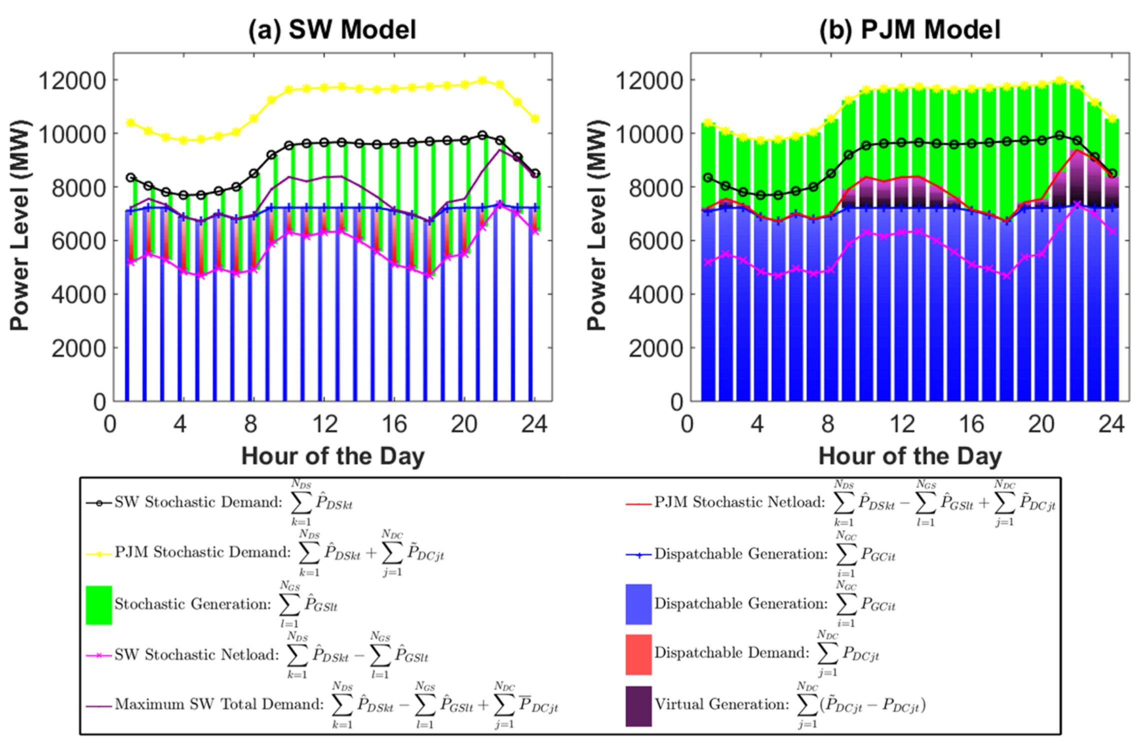

Fig. 1. Social Welfare & Industrial DSM Model Unit Commitment with Accurate Baseline

Returning to the social welfare dispatch in Figure 1a, an interesting phenomenon occurs when the stochastic generation is too low or too high. For example, in Hours 22, the stochastic generation is low and the dispatchable generation must rise to meet the stochastic netload. This shows that there is a limit to the ability of social welfare demand side management helping mitigate renewable energy down-ramp events [84]. That said, the social welfare model would still incentivize greater demand side participation in this case because it would send a long term signal that would lower the stochastic demand and stochastic net load curves. On the other hand, in Hour 18, the stochastic generation is so high that it reaches the maximum capacity of the dispatchable demand. This shows that in the case of an abundance of renewable energy, the social welfare model encourages greater demand side participation. The alternative would be to waste this energy in the form of renewable energy curtailment [84].

Industrial DSM dispatch in Figure 2b displays a similar behavior. The same hours can be studied for when the stochastic generation is too low or too high. In Hours 22, again the stochastic generation is too low and the virtual generation are running at maximum capacity. The dispatchable generation still needs to rise to meet power balance. As in the case of the social welfare model, the industrial DSM model is incapable of mitigating renewable energy down-ramp events although a long term signal for greater demand side management would be created. However, Hour 18 requires no virtual generation in the industrial DSM case. This means that when there is an abundance of renewable energy, there is no large incentive to expand demand side participation. These incentives instead occur in Hours 9-14 when the stochastic demand and baseline is high but not enough renewable energy exists to bring down the industrial DSM netload.

B. *Inflated Baseline*

The two demand side management optimization programs are now studied for their dispatch levels, social welfare values, and total system costs when the industrial DSM program is subjected to an inflated industrial baseline which is absent from the social welfare model. A 20% error was chosen to exaggerate the effects of inflated baselines [85].

1) Dispatch Levels: Figure 2 shows the SW and industrial dispatch levels where the baseline is 120% of the forecast. While the SW dispatch result remains the same, in the industrial dispatch, the industrial dispatchable generation (blue line) in Figure 2b becomes fairly constant compared to that from social welfare model in Figure 2a. In Hour 5 & 18, the industrial model shows that the virtual generation participate in maintaining a relatively constant dispatchable generation level. This is because the model assumes higher DSM participation than actually exists [85]. However, the dispatched level may not always be achievable, thus requiring more subsequent control [85].

2) Social Welfare: Making a rigorous and fair comparison between the two optimization programs requires borrowing the concepts from each optimization program and artificially applying into the domain of the other. Although the industrial DSM model does not optimize social welfare, the social welfare can still be evaluated for both cases. Figure 3 evaluates the social welfare function $(-\mathcal{W})$ for both simulations. As expected, the hourly social welfare value is highest in Hours 17-20 when the stochastic generation is high and the stochastic net load is low. In contrast, it is lowest in Hours 21-23 when the stochastic generation is low and the stochastic net load is high. Interestingly, and perhaps unintuitively, the industrial model with artificially high baseline results in "higher" social welfare values. Because the virtual generators are starting from the inflated baseline, their marginal costs accumulate more rapidly than if they had started from the true baseline. As a result, they end up demanding more as measured from zero. This artificially inflates the social welfare function perhaps beyond what is achievable. For example, in the case that the virtual generators are dispatched between 0 and 20% of the baseline, then they are being dispatched to demand *more* than the original load forecast or correct baseline value. This yields a higher social welfare value but does not have a basis in reality [85].

3) System Costs: Figure 4 now evaluates the total system cost function in Equation (15) and compares the results in a similar way. While the industrial model cost is evaluated using an inflated baseline, the social welfare model evaluates the total system cost from an error-free baseline. As expected, the cost from the industrial model is consistently higher than that from the social welfare model because it is compensating for false load reductions. The total costs for the social welfare and industrial models were $4.45 * 10^6\$$ and $5.12 * 10^6\$$ respectively. Thus, in this case the 20% error in industrial baseline lead to a 14.9% difference in the total costs [85].

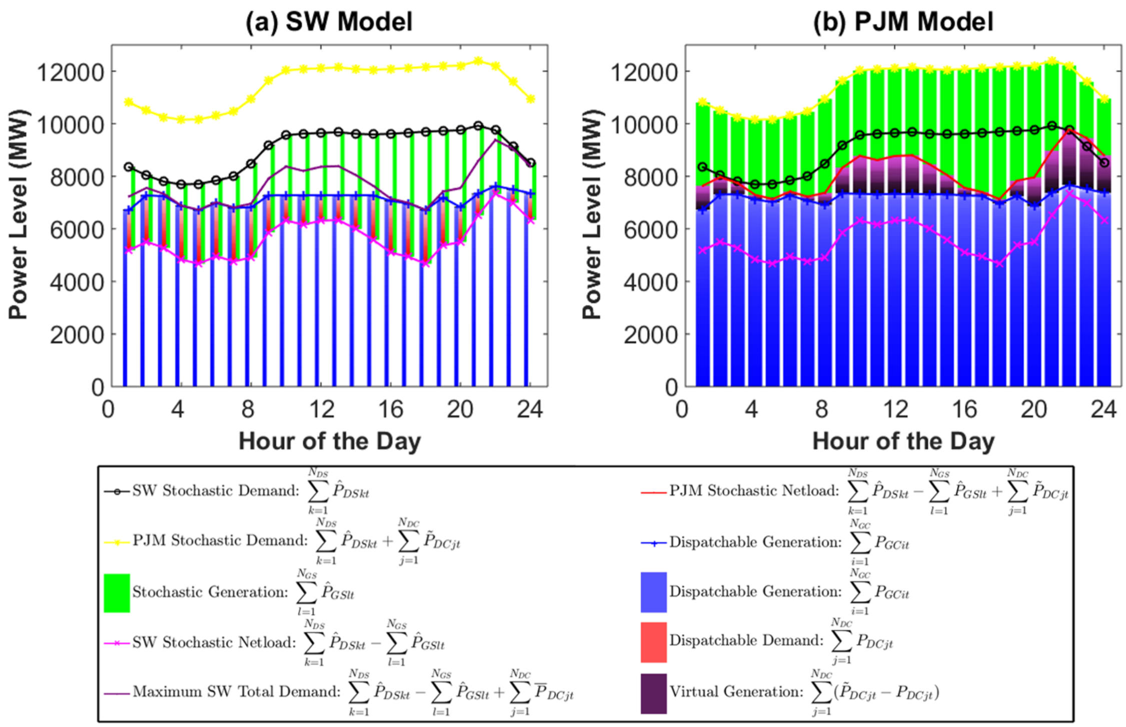

Fig. 2. Social Welfare & Industrial DSM Model Unit Commitment with Over Estimated Baseline

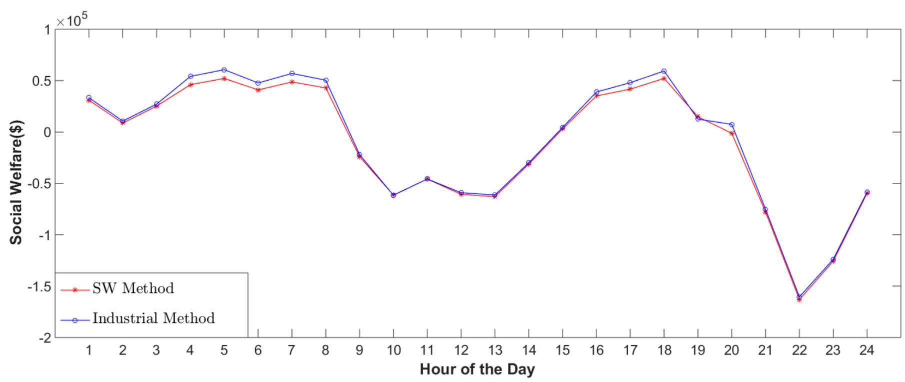

Fig. 3. Social Welfare Values for the Social Welfare & Industrial Model

VII. Conclusion

The industrial & academic literature have taken divergent approaches to demand side management implementation. While academic implementations have sought to optimize social welfare, industrial implementations optimize total costs where virtual generators are compensated for their load reduction from a predefined baseline. This work has rigorously compared the two methods using the same test case; leading to three outcomes. First, the comparison showed that while the social welfare model uses a stochastic net load composed of two terms, the industrial DSM model uses a stochastic net load composed of three terms including an additional term for the electricity consumption baseline. It is thus more prone to error because customers have the potential to artificially inflate this baseline to gain higher financial compensation for load reduction. Second, in the case that the baseline systematically rejects error, the two methods mitigate the stochastic net load in fundamentally the same way and incentivize same participation under various conditions of renewable energy integration and conventional demand, assuming the utility functions of dispatchable demands and cost functions of virtual generators are properly reconciled. This work has also compared the two models while introducing a 20% error in industrial electricity consumption baseline. As a third outcome, the comparison showed that the errors in baselines lead to different dispatch levels, higher systems costs, and

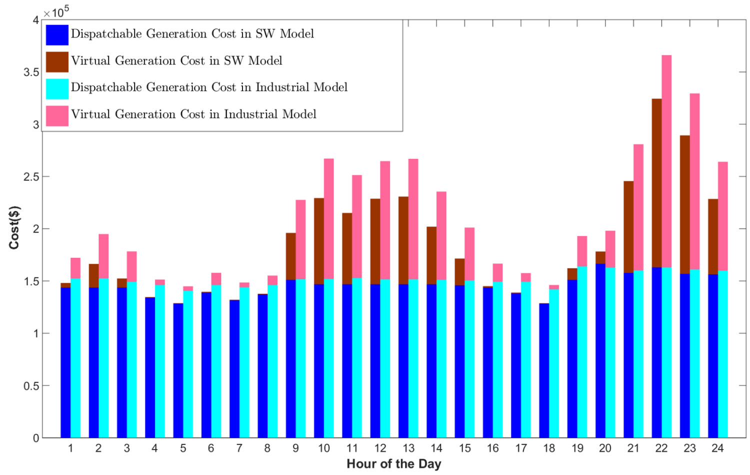

Fig. 4. System Cost in Social Welfare & Industrial DSM Models

potentially unachievable levels of social welfare. Furthermore, the erroneous baselines is also likely to require more control activity after commitment in subsequent layers of enterprise control [74], [75], [99]–[101].

ACKNOWLEDGMENT

The authors would like to thank Aramazd Muzhikyan for several insights into the implementation of this work.

REFERENCES

[1] J. Smith, M. Milligan, E. DeMeo, and B. Parsons, "Utility Wind Integration and Operating Impact State of the Art," *IEEE Transactions on Power Systems*, vol. 22, no. 3, pp. 900–908, Aug 2007.

[2] Y. T. Tan and D. S. Kirschen, "Co-optimization of Energy and Reserve in Electricity Markets with Demand-side Participation in Reserve Services," in *Power Systems Conference and Exposition, 2006. PSCE'06. 2006 IEEE PES*, October 2006, pp. 1182–1189.

[3] M. Ilic, L. Xie, and J.-Y. Joo, "Efficient Coordination of Wind Power and Price-Responsive Demand - Part I: Theoretical Foundations," *IEEE Transactions on Power Systems*, vol. 26, no. 4, pp. 1875–1884, November 2011.

[4] K. Dietrich, J. Latorre, L. Olmos, and A. Ramos, "Demand Response in an Isolated System With High Wind Integration," *IEEE Transactions on Power Systems*, vol. 27, no. 1, pp. 20–29, Feb 2012.

[5] S. Rahman and Rinaldy, "An efficient load model for analyzing demand side management impacts," *IEEE Transactions on Power Systems*, vol. 8, no. 3, pp. 1219–1226, Aug 1993.

[6] M. das Neves Queiroz de Macedo, J. J. M. Galo, L. A. L. Almeida, and A. C. C. Lima, "Opportunities and Challenges of DSM in Smart Grid Environment," *The Third International Conference on Smart Grids, Green Communications and IT Energy-aware Technologies*, pp. 156–160, 2013.

[7] D. Huang, R. Billinton, and W. Wangdee, "Effects of demand side management on bulk system adequacy evaluation," in *2010 IEEE 11th International Conference on Probabilistic Methods Applied to Power Systems (PMAPS)*, June 2010, pp. 593–598.

[8] D. Kirschen, "Demand-Side View of Electry Markets," *IEEE Transactions on Power Systems*, vol. 18, no. 2, pp. 520–527, May 2003.

[9] D. P. Chassin and Pacific Northwest National Laboratory, "How Demand Response Can Mitigate Renewable Intermittency," ser. 4th International Conference on Integration of Renewable and Distributed Energy Resources. IEEE, December 2000.

[10] L. Chen, N. Li, L. Jiang, and S. H. Low, "Optimal Demand Response: Problem Formulation and Deterministic Case," *Control and Optimization Methods for Electric Smart Grids*, vol. 3, pp. 63–85, 2012.

[11] H.-p. Chao, "Demand response in wholesale electricity markets: the choice of customer baseline," *Journal of Regulatory Economics*, vol. 39, no. 1, pp. 68–88, Nov 2011.

[12] S. Karnouskos, D. Ilic, and P. Silva, "Using flexible energy infrastructures for demand response in a Smart Grid city," in *2012 3rd IEEE PES International Conference and Exhibition on Innovative Smart Grid Technologies (ISGT Europe)*, Oct 2012, pp. 1–7.

[13] A. Rosso, J. Ma, D. S. Kirschen, and L. F. Ochoa, "Assessing the Contribution of Demand Side Management to Power System Flexibility," in *2011 50th IEEE Conference on Decision and Control and European Control Conference (CDC-ECC)*, 2011.

[14] S. Vandael, B. Claessens, M. Hommelberg, T. Holvoet, and G. Deconinck, "A Scalable Three-Step Approach for Demand Side Management of Plug-in Hybrid Vehicles," *IEEE Transactions on Smart Grid*, vol. 4, no. 2, pp. 720–728, June 2013.

[15] L. A. C. Lopes and M. Dalal-Bachi, "Economic Dispatch and Demand Side Management via Frequency Control in PV-Diesel Hybrid Mini-Grids," in *6th European Conference on PV-Hybrid and Mini-Grids, Chambery*, April 2012.

[16] C. W. Gellings, "The Concept of Demand-Side Management for Electric Utilities," in *Proceedings of the IEEE*, vol. 73, no. 10, October 1985, pp. 1468–1470.

[17] P. Palensky and D. Dietrich, "Demand Side Management: Demand Response, Intelligent Energy Systems, and Smart Loads," *IEEE Transactions on Industrial Informatics*, vol. 7, no. 3, pp. 381–388, Aug 2011.

[18] G. Strbac, "Demand side management: Benefits and challenges," *Energy Policy*, vol. 36, no. 12, pp. 4419–4426, 2008.

[19] F. M. Andersen, S. G. Jensen, H. V. Larsen, P. Meibom, H. Ravn, K. Skytte, and M. Togeby, "Analyses of Demand Response in Denmark," Tech. Rep. October, Oct 2006.

[20] J. N. Sheen, "Economic profitability analysis of demand side management program," *Energy Conversion and Management*, vol. 46, no. 18 - 19, pp. 2919 – 2935, 2005.

[21] U.S. Department of Energy, "Benefits of Demand Response in Electricity Markets and Recommendations for Achieving Them: A Report to the United States Congress Pursuant to Section 1253 of the Energy Policy Act of 2005," Tech. Rep. February, 2006.

[22] R. Walawalkar, S. Blumsack, J. Apt, and S. Fernands, "An Economic Welfare Analysis of Demand Response in the PJM Electricity Market," *Energy Policy*, vol. 36, no. 10, pp. 3692 – 3702, Oct 2008.

[23] ——, "Analyzing PJM 2019 economic demand response program," in *Power and Energy Society General Meeting - Conversion and Delivery of Electrical Energy in the 21st Century, 2008 IEEE*, July 2008, pp. 1–9.

[24] P. Centolella, "The integration of Price Responsive Demand into Regional Transmission Organization (RTO) wholesale power markets and system operations," *Energy*, vol. 35, no. 4, pp. 1568 – 1574, 2010.

[25] P. Cappers, C. Goldman, and D. Kathan, "Demand Response in U.S. Electricity Markets: Empirical Evidence," *Energy*, vol. 35, no. 4, pp. 1526 – 1535, 2010.

[26] R. Walawalkar, S. Fernands, N. Thakur, and K. R. Chevva, "Evolution and current status of demand response (DR) in electricity markets: Insights from PJM and NYISO," *Energy*, vol. 35, no. 4, pp. 1553 – 1560, 2010.

[27] L. A. Greening, "Demand response resources: Who is responsible for implementation in a deregulated market?" *Energy*, vol. 35, no. 4, pp. 1518 – 1525, 2010.

[28] Ontario Energy Board, "Demand-side Management and Demand Response in the Ontario Electricity Sector: Report of the Board to the Minister of Energy," Tech. Rep., Mar 2004.

[29] M. Fouda, Z. Fadlullah, N. Kato, A. Takeuchi, and Y. Nozaki, "A novel demand control policy for improving quality of power usage in smart grid," in *Global Communications Conference (GLOBECOM), 2012 IEEE*, Dec 2012, pp. 5154–5159.

[30] A.-H. Mohsenian-Rad, V. Wong, J. Jatskevich, R. Schober, and A. Leon-Garcia, "Autonomous Demand-Side Management Based on Game-Theoretic Energy Consumption Scheduling for the Future Smart Grid," *IEEE Transactions on Smart Grid*, vol. 1, no. 3, pp. 320–331, Dec 2010.

[31] I. Lampropoulos, P. van den Bosch, and W. Kling, "A predictive control scheme for automated demand response mechanisms," in *2012 3rd IEEE PES International Conference and Exhibition on Innovative Smart Grid Technologies (ISGT Europe)*, Oct 2012, pp. 1–8.

[32] PJM State & Member Training Dept., "PJM Demand Side Response," 2011.

[33] K. Matsumoto, Y. Takamuki, N. Mori, and M. Kitayama, "An interactive approach to demand side management based on utility functions," in *International Conference on Electric Utility Deregulation and Restructuring and Power Technologies, 2000.*, 2000, pp. 147–150.

[34] B. Ramanathan and V. Vittal, "A Framework for Evaluation of Advanced Direct Load Control With Minimum Disruption," *IEEE Transactions on Power Systems*, vol. 23, no. 4, pp. 1681–1688, Nov 2008.

[35] M. Roozbehani, M. Dahleh, and S. Mitter, "On the Stability of Wholesale Electricity Markets under Real-Time Pricing," in *2010 49th IEEE Conference on Decision and Control*, December 2010, pp. 1911–1918.

[36] ——, "Dynamic Pricing and Stabilization of Supply and Demand in Modern Electric Power Grids," in *2010 First IEEE International Conference on Smart Grid Communications*, October 2010, pp. 543–548.

[37] Z. Fadlullah, D. M. Quan, N. Kato, and I. Stojmenovic, "GTES: An Optimized Game-Theoretic Demand-Side Management Scheme for Smart Grid," *IEEE Systems Journal*, vol. 8, no. 2, pp. 588–597, June 2014.

[38] Y. Liu, C. Yuen, S. Huang, N. Ul Hassan, X. Wang, and S. Xie, "Peak-to-Average Ratio Constrained Demand-Side Management With Consumer's Preference in Residential Smart Grid," *IEEE Journal of Selected Topics in Signal Processing*, vol. 8, no. 6, pp. 1084–1097, Dec 2014.

[39] Y. Tanoto, M. Santoso, and E. Hosea, "Multi-Dimensional Assessment for Residential Lighting Demand Side Management: A Proposed Framework," *Applied Mechanics and Materials*, vol. 284-287, pp. 3612–3616, 2013.

[40] S. Bahrami, M. Parniani, and A. Vafaeimehr, "A modified approach for residential load scheduling using smart meters," in *2012 3rd IEEE PES International Conference and Exhibition on Innovative Smart Grid Technologies (ISGT Europe)*, Oct 2012, pp. 1–8.

[41] M. Mazidi, A. Zakariazadeh, S. Jadid, and P. Siano, "Integrated scheduling of renewable generation and demand response programs in a microgrid," *Energy Conversion and Management*, vol. 86, pp. 1118–1127, 2014.

[42] K. Heussen, S. You, B. Biegel, L. Hansen, and K. Andersen, "Indirect control for demand side management - A conceptual introduction," in *2012 3rd IEEE PES International Conference and Exhibition on Innovative Smart Grid Technologies (ISGT Europe)*, Oct 2012, pp. 1–8.

[43] A. Molderink, V. Bakker, J. Hurink, and G. Smit, "Comparing demand side management approaches," in *2012 3rd IEEE PES International Conference and Exhibition on Innovative Smart Grid Technologies (ISGT Europe)*, Oct 2012, pp. 1–8.

[44] S. D. Ramchurn, P. Vytelingum, A. Rogers, and N. Jennings, "Agent-based control for decentralised demand side management in the smart grid," *The Tenth International Conference on Autonomous Agents and Multiagent Systems (AAMAS 2011)*, 2011.

[45] L. Wang, Z. Wang, and R. Yang, "Intelligent Multiagent Control System for Energy and Comfort Management in Smart and Sustainable Buildings," *IEEE Transactions on Smart Grid*, vol. 3, no. 2, pp. 605–617, June 2012.

[46] B. Claessens, S. Vandael, F. Ruelens, and M. Hommelberg, "Self-learning demand side management for a heterogeneous cluster of devices with binary control actions," in *2012 3rd IEEE PES International Conference and Exhibition on Innovative Smart Grid Technologies (ISGT Europe)*, Oct 2012, pp. 1–8.

[47] V. Muenzel, J. de Hoog, I. Mareels, A. Vishwanath, S. Kalyanaraman, and A. Gort, "PV Generation and Demand Mismatch: Evaluating the Potential of Residential Storage," *The IEEE PES Conference on Innovative Smart Grid Technologies 2015*, 2015.

[48] I. Atzeni, L. Ordonez, G. Scutari, D. Palomar, and J. Fonollosa, "Demand-Side Management via Distributed Energy Generation and Storage Optimization," *IEEE Transactions on Smart Grid*, vol. 4, no. 2, pp. 866–876, June 2013.

[49] N. Adilov, R. E. Schuler, W. D. Schulze, and D. E. Toomey, "The Effect of Customer Participation in Electricity Markets: An Experimental Analysis of Alternative Market Structures," in *The 37th Hawaii International Conference on System Sciences*, 2004.
[50] The Cadmus Group, Inc. / Energy Services, "Assessment of Long-Term, System-Wide Potential for Demand-Side and Other Supplemental Resources, 2013-2032 Volume I," March 2013.
[51] C. Goldman, N. Hopper, R. Bharvirkar, B. Neenan, and P. Cappers, "Estimating Demand Response Market Potential among Large Commercial and Industrial Customers: A Scoping Study," January 2007.
[52] A. B. Haney, T. Jamasb, L. M. Platchkov, and M. G. Pollitt, "Demand-side Management Strategies and the Residential Sector: Lessons from International Experience," November 2010.
[53] K. Spees and L. B. Lave, "Demand response and electricity market efficiency," *The Electricity Journal*, vol. 20, no. 3, pp. 69–85, 2007.
[54] S. Neumann, F. Sioshansi, A. Vojdani, and G. Yee, "How to get more response from demand response," *The Electricity Journal*, vol. 19, no. 8, pp. 24–31, 2006.
[55] A. Zibelman and E. N. Krapels, "Deployment of demand response as a real-time resource in organized markets."
[56] J. Wu, X. Guan, F. Gao, and G. Sun, "Social Welfare Maximization Auction for Electricity Markets with Elastic Demand," in *7th World Congress on Intelligent Control and Automation, 2008. WCICA 2008*, ser. Proceedings of the World Congress on Intelligent Control and Automation (WCICA). Institute of Electrical and Electronics Engineers Inc., June 2008, pp. 7157–7162.
[57] L. Na, L. Chen, and S. H. Low, "Optimal demand response based on utility maximization in power networks," in *2011 IEEE Power and Energy Society General Meeting*, ser. IEEE Power and Energy Society General Meeting. IEEE Computer Society, July 2011, pp. 1–8.
[58] FERC, "Final Rule, Order 719, Wholesale Competition in Regions with Organized Electric Markets," FERC, Tech. Rep., 2008.
[59] ——, "2012 Assessment of Demand Response and Advanced Metering," FERC, Tech. Rep., 2012.
[60] J. Torriti, M. G. Hassan, and M. Leach, "Demand response experience in Europe: Policies, programmes and implementation," *Energy*, vol. 35, no. 4, pp. 1575–1583, 2010.
[61] M. H. Albadi and E. F. El-Saadany, "A summary of demand response in electricity markets," *Electric Power Systems Research*, vol. 78, no. 11, pp. 1989 – 1996, 2008.
[62] H. Zhong, L. Xie, and Q. Xia, "Coupon Incentive-Based Demand Response: Theory and Case Study," in *IEEE Transactions on Power Systems*, 2013.
[63] K. Herter and S. Wayland, "Residential response to critical-peak pricing of electricity: California evidence," *Energy*, vol. 35, no. 4, pp. 1561 – 1567, 2010.
[64] N. Ruiz, I. Cobelo, and J. Oyarzabal, "A Direct Load Control Model for Virtual Power Plant Management," *IEEE Transactions on Power Systems*, vol. 24, no. 2, pp. 959–966, May 2009.
[65] E. Karangelos and F. Bouffard, "Towards Full Integration of Demand-Side Resources in Joint Forward Energy/Reserve Electricity Markets," *IEEE Transactions on Power Systems*, vol. 27, no. 1, pp. 280–289, Feb 2012.
[66] E. Almeshaiel and H. Soltan, "A Methodology for Electric Power Load Forecasting," *Alexandria Engineering Journal*, vol. 50, pp. 137–144, June 2011.
[67] EnerNOC, "The Demand Response Baseline," Tech. Rep., 2009.
[68] K. Coughlin, M. A. Piette, C. Goldman, and S. Kiliccote, "Estimating Demand Response Load Impacts: Evaluation of Baseline Load Models for Non Residential Buildings in California," January 2008.
[69] KEMA, "PJM Empirical Analysis of Demand Response Baseline Methods," Tech. Rep., April 2011.
[70] M. L. Goldberg, G. K. Agnew, and D. Kema, "Measurement and Verification for Demand Response," Tech. Rep., February 2013.
[71] J. Bushnell, B. F. Hobbs, and F. A. Wolak, "When it comes to demand response, is FERC its own worst enemy?" *The Electricity Journal*, vol. 22, no. 8, pp. 9–18, 2009.
[72] NYISO, "Wholesale vs.Retail Electricity." [Online]. Available: http://www.nyiso.com/public/about_nyiso/understanding_the_markets/wholesale_retail/index.jsp
[73] PJM, "PJM Markets & Operations Demand Response." [Online]. Available: http://www.pjm.com/markets-and-operations/demand-response.aspx
[74] A. Muzhikyan, A. M. Farid, and K. Youcef-Toumi, "An Enterprise Control Assessment Method for Variable Energy Resource Induced Power System Imbalances Part 1: Methodology," *IEEE Transactions on Industrial Electronics*, vol. 62, no. 4, pp. 2448–2458, 2015. [Online]. Available: http://amfarid.scripts.mit.edu/resources/Journals/SPG-J15.pdf
[75] ——, "An Enterprise Control Assessment Method for Variable Energy Resource Induced Power System Imbalances Part 2: Results," *IEEE Transactions on Industrial Electronics*, vol. 62, no. 4, pp. 2459 – 2467, 2015. [Online]. Available: http://amfarid.scripts.mit.edu/resources/Journals/SPG-J16.pdf
[76] X. Zou, "Double-sided auction mechanism design in electricity based on maximizing social welfare," *Energy Policy*, vol. 37, no. 11, pp. 4231 – 4239, 2009.
[77] M. Govardhan and R. Roy, "Impact of demand side management on unit commitment problem," in *2014 International Conference on Control, Instrumentation, Energy and Communication (CIEC)*, Jan 2014, pp. 446–450.
[78] Y. Ikeda, T. Ikegami, K. Kataoka, and K. Ogimoto, "A Unit Commitment Model with Demand Response for the Integration of Renewable Energies," in *2012 IEEE Power and Energy Society General Meeting*, 2011.
[79] "Robust unit commitment problem with demand response and wind energy, author = Long Zhao and Bo Zeng," *2012 IEEE Power and Energy Society General Meeting*, pp. 1–8, 2012.
[80] H. Wu, M. Shahidehpour, and A. Al-Abdulwahab, "Hourly demand response in day-ahead scheduling for managing the variability of renewable energy," *IET Generation, Transmission & Distribution*, pp. 226–234, 2013.
[81] M. Kia, M. M. R. Sahebi, E. A. Duki, and S. H. Hosseini, "Simultaneous Implementation of Optimal Demand Response and Security Constrained Unit Commitment," in *2011 16th Conference on Electrical Power Distribution Networks (EPDC)*, 2011.
[82] J. Hurink, M. Bossman, A. Molderink, V. Bakker, and G. Smith, "Modeling, Simulation, and Optimization for the 21st Century Electric Power Grid," in *Engineering Conferences International*, 2012.

[83] F. Schneider, D. Klabjan, and U. W. Thonemann, "Incorporating Demand Response with Load Shifting into Stochastic Unit Commitment," April 2013.

[84] B. Jiang, A. Farid, and K. Youcef-Toumi, "A Comparison of Day-Ahead Wholesale Market: Social Welfare vs Industrial Demand Side Management," in *2015 IEEE International Conference on Industrial Technology*, March 2015.

[85] ——, "Impacts of Industrial Baseline Errors on Costs & Social Welfare in the Demand Side Management of Day-Ahead Wholesale Markets (in press)," *2015 ASME Power & Energy Conference*, 2015.

[86] A. Gomez-Exposito, A. J. Conejo, and C. Canizares, *Electric Energy Systems: Analysis and Operation*. Boca Raton, FL: CRC Press, 2008.

[87] C. Harris, J. P. Meyers, and M. E. Webber, "A unit commitment study of the application of energy storage toward the integration of renewable generation," *Journal of Renewable and Sustainable Energy*, vol. 4, no. 1, p. 013120 (20 pp.), Jan 2012. [Online]. Available: http://dx.doi.org/10.1063/1.3683529

[88] B. F. Hobbs, M. H. Rothkopf, R. P. ONeill, and H.-p. Chao, *The Next Generation of Electric Power Unit Commitment Models*. New York, NY, USA: Kluwer Academic Publishers, 2001.

[89] M. Nazari, M. Ardehali, and S. Jafari, "Pumped-storage unit commitment with considerations for energy demand, economics, and environmental constraints," *Energy*, vol. 35, no. 10, pp. 4092–4101, Oct 2010.

[90] T. Senjyu, T. Miyagi, S. A. Yousuf, N. Urasaki, and T. Funabashi, "A technique for unit commitment with energy storage system," *International Journal of Electrical Power & Energy Systems*, vol. 29, no. 1, pp. 91–98, Jan 2007. [Online]. Available: http://dx.doi.org/10.1016/j.ijepes.2006.05.004

[91] L. Wu, M. Shahidehpour, and T. Li, "Stochastic security-constrained unit commitment," *IEEE Trans. Power Syst.*, vol. 22, no. 2, pp. 800–811, May 2007.

[92] T. J. Brennan, "Demand-Side Management Programs Under Retail Electricity Competition," 1998.

[93] Y. Fu, M. Shahidehpour, and Z. Li, "Security-constrained unit commitment with ac constraints," *IEEE Transactions on Power Systems*, vol. 20, no. 2, pp. 1001–1013, 2005.

[94] C. Grigg, P. Wong, P. Albrecht, R. Allan, M. Bhavaraju, R. Billinton, Q. Chen, C. Fong, S. Haddad, S. Kuruganty, W. Li, R. Mukerji, D. Patton, N. Rau, D. Reppen, A. Schneider, M. Shahidehpour, and C. Singh, "The IEEE Reliability Test System-1996. A report prepared by the Reliability Test System Task Force of the Application of Probability Methods Subcommittee," *IEEE Transactions on Power Systems*, vol. 14, no. 3, pp. 1010–1020, 1999.

[95] U.S. Energy Information Administration, "Short-Term Energy Outlook," November 2014.

[96] BPA, "Data for BPA Balancing Authority Total Load, Wind Gen, Wind Forecast, Hydro, Thermal, and Net Interchange," 2014. [Online]. Available: http://transmission.bpa.gov/business/operations/wind/

[97] ——, "Wind Power Forecasting Data," 2014. [Online]. Available: http://www.bpa.gov/Projects/Initiatives/Wind/Pages/Wind-Power-Forecasting-Data.aspx

[98] "CPLEX," *GAMS - The Solver Manuals*, vol. 12. [Online]. Available: www.gams.com/dd/docs/solvers/cplex

[99] A. Farid and A. Muzhikyan, "The Need for Holistic Assessment Methods for the Future Electricity Grid," in *GCC CIGRE Power*, 2013, pp. 1–12.

[100] A. Muzhikyan, A. Farid, and K. Youcef-Toumi, "Variable Energy Resource Induced Power System Imbalances: A Generalized Assessment Approach," in *2013 1st IEEE Conference on Technologies for Sustainability (SusTech)*, 2013, pp. 1–8.

[101] ——, "Variable Energy Resource Induced Power System Imbalances: Mitigation by Increased System Flexibility, Spinning Reserves and Regulation," in *2013 1st IEEE Conference on Technologies for Sustainability (SusTech)*, Aug 2013, pp. 15–22.